Classification of three-phase power disturbances based on model order selection in smart grid applications

Zakarya Oubrahim, Vincent Choqueuse, Yassine Amirat, Mohamed Benbouzid

Classification of Three-Phase Power Disturbances based on Model Order Selection in Smart Grid Applications

Zakarya Oubrahim[1,2], Vincent Choqueuse[1], Yassine Amirat[2], and Mohamed Benbouzid[1,3]
[1] University of Brest, FRE CNRS 3744 IRDL, Brest, France
[2] ISEN Brest, FRE CNRS 3744 IRDL, Brest, France
[3] Shanghai Maritime University, Shanghai, China
Email: zakarya.oubrahim@univ-brest.fr, vincent.choqueuse@univ-brest.fr
yassine.amirat@isen.fr, and mohamed.benbouzid@univ-brest.fr

***Abstract*—This paper deals with a new classification techniques for power quality analysis. Specifically, the proposed technique aims at discriminating between four classes, where each class depends on the number of non-zero symmetrical components. By reformulating the classification problem as a pure model order selection one, we propose a classifier based on Information Theoretical Criteria. It yields the highest statistical performances. The performances of this proposed classifier are evaluated using Monte Carlo simulations with synthetic three-phase signals. Simulation results illustrate the effectiveness of the proposed classifier for power quality disturbances classification.**

***Index Terms*—Power Quality Disturbances, Detection and Classification, Symmetrical Components, Unbalanced Power System, Smart Grid Monitoring.**

I. Introduction

In the last decade, renewable energy sources have undergone a rapid expansion due to the growing need for cleaner and more sustainable energies [1]–[6]. Despite its ecological benefit, the massive introduction of intermittent and decentralized renewable energy sources in the energy mix has raised new technical challenges. For example, the use of intermittent energy sources may introduce grid instability that can lead, in the worst case, to the system blackout. To overcome this difficulty, modern energy management systems continuously monitor the grid state and trigger appropriate operations is needed. These modern systems relies on the combination of information and communication technologies with power electronic engineering, and they are usually subsumed under the generic term of ”smart grid”.

This work was supported by Brest Métropole and ISEN Brest.

A key role of a smart grid is to allow the electrical grid to be more flexible, more efficient, and meeting Power Quality standards. Among these requirements, Power Quality (PQ) is of main concern since any disturbance can prevent end-user equipment from operating properly [7]. PQ disturbances can have different characteristics and consequences for end-user equipments. They are usually divided into several classes such as sag, swell, transient, fluctuation, and interruption [7]. Voltage sags and swells are the most important events in voltage supply because they can degrade the performance and efficiency of customer loads. In particular, voltage sags and swells can lead to various problems such as instabilities and failure of electrical equipments, and can produce million-dollar losses in commercial and industrial consumers [8]. To minimize their economical impacts, it becomes imperative to integrate advanced algorithms for the detection and classification of voltage sags and swells.

Several techniques have been proposed in the literature to detect three-phase unbalance and/or classify voltage sags and swells. Regarding the detection of three-phase unbalance, the references [1], [9] describe two techniques based on hypothesis tests. The classification of PQ disturbances have also been investigated in several papers [10]–[14]. In [10] and [13], two voltage classifiers based on symmetrical components (S-C) and three-phase voltage magnitudes and their phase angles (TP-TA) are respectively proposed. Both classifiers identify the six voltage sags type C_a, C_b, C_c, D_a, D_b, and D_c [10]. The classifier described in [10], [11] compares the six RMS values of phase and phase-to-phase voltages after removing the zero sequence component. this six-phases classifier identifies also voltage sags type C_a, C_b, C_c, D_a,

D_b, and D_c. Despite their simplicity, these techniques are very sensitive to large variations in magnitude or phase-angle jump under various voltage unbalance conditions and they do not cover all sags types proposed in [15]. In [16], the authors have proposed a technique based on space vector representation in the complex plane and zero sequence voltage. This technique provides a complete dip and swell type classification. Other classifiers based on pattern recognition techniques, such as Artificial Network or Support Vector Machine, have also been presented in [17]–[23]. However, these supervised classifiers have relative high computational complexity and their performances critically depend on the quality and size of the training database.

This paper proposes a new method devoted for PQ disturbance classification. Similarly to the technique described in [9], the proposed classifier is based on model order selection [24]. Nevertheless, while the method in [9] mainly focuses on the detection problem, the proposed technique addresses the classification one. Specifically, the proposed classifier is able to identify the number of non-zero symmetrical components, and to classify the signal into 4 classes. The first class includes signals with both null zero- and negative-sequences. The second and third class include signals with null zero- and negative-sequence, respectively. Finally, the fourth class includes signals with non-null symmetrical components.

II. Signal Model and Classification

This section presents the three-phase signal and phasor models. Based on the phasor model, we also describe the proposed 4-classes classification.

A. Three-Phase Signals Model

In a three-phase power system, the signal on phase m ($m = 0, 1, 2$) can be expressed as [25]

$$x_m[n] = a_m \cos(nw_0 + \varphi_m) + b_m[n], \tag{1}$$

where a_m and φ_m correspond to the amplitude and phase angle, respectively, ω_0 denotes the normalized angular frequency, and $b_m[n]$ refers to the additive noise. The parameters a_m and φ_m are usually described more compactly by introducing the complex phasor. Mathematically, the phasor on phase m is defined as

$$c_m \triangleq a_m e^{j\varphi_m}. \tag{2}$$

Without loss of generality, we assume that the voltage sensors record N consecutive samples ($n = 0, 1 \cdots, N-1$). By using a matrix form, the recorded samples can be written as

$$\mathbf{x} = (\mathbf{I}_{33} \otimes \mathbf{A})\, \tilde{\mathbf{c}} + \mathbf{b}, \tag{3}$$

where $\otimes$ corresponds to the Kronecker product and

- $\mathbf{x}$ and $\mathbf{b}$ are $3N \times 1$ column vectors that correspond to the recorded and noise samples, respectively. These vectors are defined as

$$\mathbf{x} = \begin{bmatrix} x_0[0] \\ \vdots \\ x_0[N-1] \\ x_1[0] \\ \vdots \\ x_1[N-1] \\ x_2[0] \\ \vdots \\ x_2[N-1] \end{bmatrix} \quad \mathbf{b} = \begin{bmatrix} b_0[0] \\ \vdots \\ b_0[N-1] \\ b_1[0] \\ \vdots \\ b_1[N-1] \\ b_2[0] \\ \vdots \\ b_2[N-1] \end{bmatrix}, \tag{4}$$

- $\mathbf{A} \triangleq [\Re e(\mathbf{a}_k)\ \ \Im m(\mathbf{a}_k)]$ is a $N \times 2$ real-valued matrix where $\mathbf{a}_k$ is a $N \times 1$ complex-values column vector defined as

$$\mathbf{a}_k = \begin{bmatrix} 1 \\ e^{jw_0} \\ \vdots \\ e^{j(N-1)w_0}. \end{bmatrix} \tag{5}$$

- $\tilde{\mathbf{c}}$ is a 6×1 real-valued column vector depending on the unknown phasors c_0, c_1, and c_2. This vector is defined as

$$\tilde{\mathbf{c}} = \begin{bmatrix} a_0 \cos(\varphi_0) \\ -a_0 \sin(\varphi_0) \\ a_1 \cos(\varphi_1) \\ -a_1 \sin(\varphi_1) \\ a_2 \cos(\varphi_2) \\ -a_2 \sin(\varphi_2) \end{bmatrix}. \tag{6}$$

B. Phasor Model

It is usually convenient to decompose the three complex phasors into a more synthetic base. In this subsection, we propose to decompose the phasors c_0, c_1, and c_2 into a basic composed of 3 symmetrical components called: the zero-sequence, z_0, positive-sequence, z_1, and negative-sequence, z_2. The three phasors can be expressed according to the three symmetrical components through the Fortescue Transform as

$$\begin{bmatrix} c_0 \\ c_1 \\ c_2 \end{bmatrix} = \begin{bmatrix} 1 & 1 & 1 \\ 1 & e^{4j\pi/3} & e^{2j\pi/3} \\ 1 & e^{2j\pi/3} & e^{4j\pi/3} \end{bmatrix} \begin{bmatrix} z_0 \\ z_1 \\ z_2 \end{bmatrix}. \quad (7)$$

The main benefit of the symmetrical components relies on the fact that, under nominal conditions and balanced faults, the symmetrical components are sparse i.e. $z_0 = z_2 = 0$. Based on the symmetrical components, we consider 4 different classes:

- $\mathcal{C}_1$: The zero and negative sequences are equal to 0 i.e. $z_0 = z_2 = 0$.
- $\mathcal{C}_2$: The zero sequence is equal to 0 i.e. $z_0 = 0$.
- $\mathcal{C}_3$: The negative sequence is equal to 0 i.e. $z_2 = 0$.
- $\mathcal{C}_4$: All sequences are different from 0.

For the 4 proposed classes, the real-valued vector containing the real and imaginary parts of the three phasors in (3) can also be expressed according to the real and imaginary parts of the symmetrical components. Indeed, the vector $\tilde{\mathbf{c}}$ can be expressed as

$$\tilde{\mathbf{c}} = \mathbf{W}_k \tilde{\mathbf{s}}_k, \quad (8)$$

where $\mathbf{W}_k$ and $\tilde{\mathbf{s}}_k$ depend on the class number. The expressions of $\mathbf{W}_k$ and $\tilde{\mathbf{s}}_k$ for the classes $\mathcal{C}_1$, $\mathcal{C}_2$, $\mathcal{C}_3$, and $\mathcal{C}_4$ are provided in Table I, where $\mathbf{Q}_k$ are 2×2 matrices defined by

$$\mathbf{Q}_k = \begin{bmatrix} \Re e(e^{2jk\pi/3}) & \Im m(e^{2jk\pi/3}) \\ \Im m(e^{2jk\pi/3}) & -\Re e(e^{2jk\pi/3}) \end{bmatrix}. \quad (9)$$

C. General Signal Model

By using (3) and (8), the signal model can be described under the general form

$$\mathbf{x} = \mathbf{M}_k \tilde{\mathbf{s}}_k + \mathbf{b}, \quad (10)$$

where k corresponds to the class number and

$$\mathbf{M}_k = (\mathbf{I}_{33} \otimes \mathbf{A})\, \mathbf{W}_k. \quad (11)$$

The goal of this paper is to estimate the class number, k ($k = 1, 2, 3, 4$), from the three-phase signal $\mathbf{x}$. To estimate k, we assume that the additive noise is Gaussian distributed with a zero mean and variance equal to σ^2 i.e. $\mathbf{b} \sim \mathcal{N}(\mathbf{0}, \sigma^2 \mathbf{I}_{3N})$. As the different signal classes are nested, we propose to reformulate the estimation problem as a pure model order selection problem. In our context, the model order refers to the size of the vector $\tilde{\mathbf{s}}_k$. Specifically, the size of the vector $\tilde{\mathbf{s}}_k$ is equal to 2 for the class $\mathcal{C}_1$, 4 for the classes $\mathcal{C}_2$ and $\mathcal{C}_3$, and 6 for the class $\mathcal{C}_4$.

TABLE I

EXPRESSIONS OF $\mathbf{W}_k$ AND $\tilde{\mathbf{s}}_k$ WITH RESPECT TO THE CLASS $\mathcal{C}_k$.

Class	$\mathcal{C}_1$	$\mathcal{C}_2$	$\mathcal{C}_3$	$\mathcal{C}_4$
k	1	2	3	4
$\mathbf{W}_k$	$\begin{bmatrix} \mathbf{Q}_0 \\ \mathbf{Q}_1 \\ \mathbf{Q}_2 \end{bmatrix}$	$\begin{bmatrix} \mathbf{Q}_0 & \mathbf{Q}_0 \\ \mathbf{Q}_1 & \mathbf{Q}_2 \\ \mathbf{Q}_2 & \mathbf{Q}_1 \end{bmatrix}$	$\begin{bmatrix} \mathbf{Q}_0 & \mathbf{Q}_0 \\ \mathbf{Q}_0 & \mathbf{Q}_1 \\ \mathbf{Q}_0 & \mathbf{Q}_2 \end{bmatrix}$	$\begin{bmatrix} \mathbf{Q}_0 & \mathbf{Q}_0 & \mathbf{Q}_0 \\ \mathbf{Q}_0 & \mathbf{Q}_1 & \mathbf{Q}_2 \\ \mathbf{Q}_0 & \mathbf{Q}_2 & \mathbf{Q}_1 \end{bmatrix}$
$\tilde{\mathbf{s}}_k$	$\begin{bmatrix} \Re e(z_1) \\ \Im m(z_1) \end{bmatrix}$	$\begin{bmatrix} \Re e(z_1) \\ \Im m(z_1) \\ \Re e(z_2) \\ \Im m(z_2) \end{bmatrix}$	$\begin{bmatrix} \Re e(z_0) \\ \Im m(z_0) \\ \Re e(z_1) \\ \Im m(z_1) \end{bmatrix}$	$\begin{bmatrix} \Re e(z_0) \\ \Im m(z_0) \\ \Re e(z_1) \\ \Im m(z_1) \\ \Re e(z_2) \\ \Im m(z_2) \end{bmatrix}$

III. CLASSIFIER BASED ON MODEL ORDER SELECTION

In this section, we describe the proposed classifier for the estimation of the class number k. This classifier is based on model order selection algorithms. Most of model order selection algorithms is based on Information theoretic Criterion [24]. Using Information Theoretic Criterion, the selected class number k is the one that minimizes the following penalized likelihood function [26]

$$\widehat{k} = \arg \min_{k=1,2,3,4} -2 \ln p(\mathbf{x}, \widehat{\tilde{\mathbf{s}}}_k) + \gamma_k, \quad (12)$$

where $\ln p(\mathbf{x}, \widehat{\tilde{\mathbf{s}}}_k)$ denotes the log-likelihood function of the measurements $\mathbf{x}$ for the class k evaluated by replacing $\mathbf{s}_k$ by its Maximum Likelihood Estimator $\widehat{\tilde{\mathbf{s}}}_k$. The term γ_k is a penalty function that depends on the total number of samples and estimated parameters. In the following paragraphs, we provide explicit expressions for the log-likelihood function and penalty terms.

A. Expression of $\ln p(\boldsymbol{x}, \widehat{\tilde{\boldsymbol{s}}}_k)$

Under the assumption of a Gaussian noise, it has been demonstrated in [24] that the log-likelihood function $\ln p(\mathbf{x}, \widehat{\tilde{\mathbf{s}}}_k)$ is equal to

$$-2 \ln p(\mathbf{x}, \widehat{\tilde{\mathbf{s}}}_k) = \text{constant} + N \ln \widehat{\sigma}_k^2, \quad (13)$$

where $\widehat{\sigma}_k^2$ is the Maximum Likelihood Estimator of the noise variance under the assumption that the signal comes from the class $\mathcal{C}_k$. The estimator of the noise variance is given by

$$\widehat{\sigma}_k^2 = \frac{1}{N} ||\tilde{\mathbf{x}} - \mathbf{M}_k \widehat{\tilde{\mathbf{s}}}_k||^2, \quad (14)$$

TABLE II
PENALTY FUNCTION WITH RESPECT TO THE CLASS $\mathcal{C}_k$.

Class	$\mathcal{C}_1$	$\mathcal{C}_2$	$\mathcal{C}_3$	$\mathcal{C}_4$
n_k	3	5	5	7
γ_k^{AIC}	6	10	10	14
γ_k^{BIC}	$3\ln(3N)$	$5\ln(3N)$	$5\ln(3N)$	$7\ln(3N)$

where $\widehat{\tilde{\mathbf{s}}}_k$ corresponds to the Maximum Likelihood Estimator of the vector $\tilde{\mathbf{s}}_k$. As $\widehat{\tilde{\mathbf{s}}}_k = (\mathbf{M}_k^T\mathbf{M}_k)^{-1}\mathbf{M}_k^T\tilde{\mathbf{s}}_k$, it follows that

$$\widehat{\sigma}_k^2 = \mathbf{x}^T\mathbf{P}_k^{\perp}\mathbf{x}, \tag{15}$$

where $\mathbf{P}_k^{\perp}$ is the orthogonal projection matrix that projects any vector $\mathbf{x}$ onto the space orthogonal to that spanned by the columns of $\mathbf{M}_k$. This orthogonal projector is defined as

$$\mathbf{P}_k^{\perp} \triangleq \mathbf{I}_{3N} - \mathbf{M}_k\left(\mathbf{M}_k^T\mathbf{M}_k\right)^{-1}\mathbf{M}_k^T. \tag{16}$$

B. Expression of γ_k

The objective of the penalty term γ_k is to encourage simplicity over complexity. Mathematically, this function penalizes the log-likelihood function with respect to the number of estimated parameters, n_k, and the number of samples, M. Several penalty terms have been proposed in the literature based on different motivations [24]. In the study, we evaluate the performance of the two following penalty terms:

– The Akaike Information Criterion (AIC)

$$\gamma_k^{AIC} = 2n_k. \tag{17}$$

– The Bayesian Information Criterion (BIC)

$$\gamma_k^{BIC} = n_k\ln(M). \tag{18}$$

In the considered model order selection problem, the number of samples is equal to $M = 3N$. Furthermore, for the class k, the number of estimated parameters is equal $l_k + 1$ where the first term is equal to the size of $\tilde{\mathbf{s}}_k$ and the second term refers to the estimation of the noise variance. Finally, the values of the AIC and BIC criteria for the class $\mathcal{C}_1$, $\mathcal{C}_2$, $\mathcal{C}_3$, and $\mathcal{C}_4$ are summed up in Table II.

C. Proposed Classifier

Based on the previous subsections, we propose a classifier for selecting the appropriate model. This classifier is called the ML classifier and it is obtained by using the exact orthogonal projector $\mathbf{P}_k^{\perp}$ in (16).

Finally, by using (13) and (15) in (12) and dropping the terms that do not depend on k, the class number $\widehat{k}$ estimated with the ML classifier is given by

$$\widehat{k}^{ML} = \arg\min_{k=1,2,3,4} N\ln\left(\mathbf{x}^T\mathbf{P}_k^{\perp}\mathbf{x}\right) + \gamma_k. \tag{19}$$

For the proposed classifier, the AIC or BIC penalty term can be used (see Table II). Finally, it is worth mentioning that the proposed classifier is also able to discriminate between classes with the same number of estimated parameters such as $\mathcal{C}_2$ and $\mathcal{C}_3$. Indeed, when two classes have the same number of estimated parameters, the estimation of the noise variance, which is contained in the log term, provides a simple measure of the goodness of fit.

IV. SIMULATION RESULTS

In this section, the performance of the proposed classifier is compared with synthetic signals generated from Matlab. Its performance is evaluated using both the AIC or BIC penalty term.

The performance of the ML classifier is quantified through the average probability of correct detection. The average probability of correct detection is estimated using $N_{mc} = 1500$ Monte Carlo simulations for each class. In each simulation, the signal is generated from the model defined in (1) with $\omega_0 = 2\pi f_0/F_s$, where the fundamental frequency $f_0 = 50Hz$ and the sampling frequency $F_s = 48 * f_0 = 2400Hz$. Amplitudes and initial phases parameters of the three-phase power system are given by Table III. Then, the average probability of correct detection is estimated as follows

$$\widehat{\mathcal{P}}_a = \frac{1}{4N_{mc}}\sum_{k=1}^{4}\sum_{n=1}^{N_c}\delta(k - \widehat{k}[n]), \tag{20}$$

where $\widehat{k}[n]$ is the estimated class for the n^{th} trial and $\delta(l)$ is the Kronecker delta which is equal to 1 if $l = 1$ and zero elsewhere. In the next subsections, the average probability of correct detection is analyzed for different signal lengths, N, and Signal to Noise Ratio (SNR) where the SNR is defined as

$$\eta = \frac{1}{6\sigma^2}\sum_{k=0}^{2}a_k^2. \tag{21}$$

A. Average Probability of Correct Detection Versus Number of Samples

Figure 1 shows the influence of the number of samples on the average probability of correct detection when the

TABLE III
SIMULATION PARAMETERS

	$\mathcal{C}_1$	$\mathcal{C}_2$	$\mathcal{C}_3$	$\mathcal{C}_4$
a_0	0.5	1	0.5	1
a_1	0.5	0.66	1.32	0.5
a_2	0.5	0.66	1.32	0.5
φ_0	$-20°$	$-20°$	$-20°$	$-20°$
φ_1	$-140°$	$-159.10°$	$-159.10°$	$-140°$
φ_2	$100°$	$119.11°$	$119.11°$	$100°$

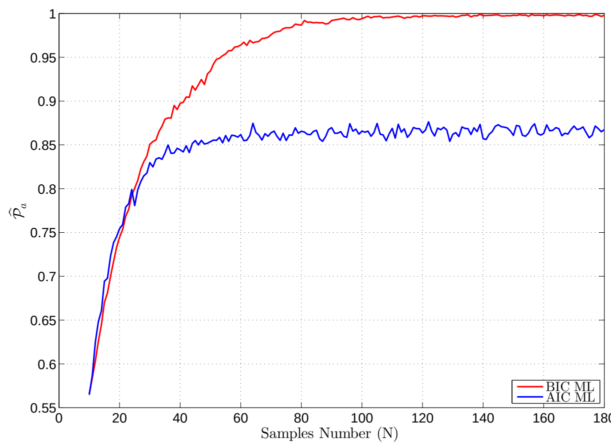

Fig. 1. Average probability of correct detection versus samples number for $SNR = 15dB$.

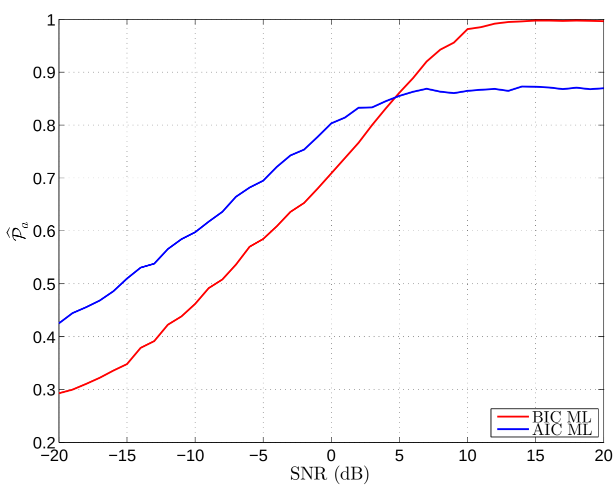

Fig. 2. Average probability of correct detection versus SNR for $N = 128$.

SNR is equal to $SNR = 15dB$. We observe that the performance of the proposed classifier increases as the samples number increases.

Regarding the penalty factors, we observe that for large N BIC penalty term lead to an average probability of correct classification equal to 1. For the AIC classifier, we observe that $\widehat{P}_a$ is not exactly equal to 1 even for large N. For small N, we also note that the AIC has a faster response time than the BIC penalty term.

B. Average Probability of Correct Detection Versus Signal to Noise Ratio

Figure 2 presents the influence of the SNR on $\widehat{P}_a$. In this simulation, the number of samples $N = 128$. For the BIC ML classifier, we see that the average probability of correct detection is equal to 1 when the SNR is large. For the AIC classifier, we observe that $\widehat{P}_a$ is not exactly equal to 1 even for large SNRs.

V. CONCLUSION

This paper dealt with the classification of power quality disturbances in three-phase unbalanced power systems. The proposed classifier is based on Information Theoretical Criteria and can discriminate between 4 classes, where each class has a particular number of non-zero symmetrical components.

Simulation results have shown that among the two considered Information Theoretical Criteria, the BIC one outperforms the AIC in terms of average probability of correct detection for a large number of samples and SNRs.

The implementation of the proposed classifier requires the use of linear algebra libraries for matrix inversion. Future work will be directed to the reduction of the computational complexity by using a suboptimal symmetrical components estimator.

REFERENCES

[1] M. Sun, S. Demirtas, and Z. Sahinoglu, "Joint voltage and phase unbalance detector for three phase power systems," *IEEE Signal Processing Letters*, vol. 20, no. 1, pp. 11–14, January 2013.

[2] H. Gharavi and R. Ghafurian, *Smart grid: The electric energy system of the future*. IEEE Press, June 2011.

[3] A. R. Bergen, *Power Systems Analysis*. Pearson Education India, July 2000.

[4] K. D. McBee and M. G. Simoes, "Utilizing a smart grid monitoring system to improve voltage quality of customers," *IEEE Transactions on Smart Grid*, vol. 3, no. 2, pp. 738–743, June 2012.

[5] IEEE, "IEEE approved draft guide for the interoperability of energy storage systems integrated with the electric power infrastructure," *IEEE P2030.2/D9.0*, pp. 1–136, June 2015.

[6] S. Amin and B. Wollenberg, "Toward a smart grid: power delivery for the 21st century," *IEEE Power and Energy Magazine*, vol. 3, no. 5, pp. 34–41, September 2005.

[7] M. H. Bollen, I. Y. Gu, S. Santoso, M. Mcgranaghan, P. A. Crossley, M. V. Ribeiro, and P. P. Ribeiro, "Bridging the gap between signal and power," *IEEE Signal Processing Magazine*, vol. 26, no. 4, pp. 12, July 2009.

[8] M. F. McGranaghan, D. R. Mueller, and M. J. Samotyj, "Voltage sags in industrial systems," *IEEE Transactions on industry applications*, vol. 29, no. 2, pp. 397–403, March-April 1993.

[9] T. Routtenberg and L. Tong, "Networked detection of voltage imbalances for three-phase power systems," in *Proceedings of the 2015 IEEE ISIE, Buzios-Rio de janiero (Brazil)*, pp. 1345–1350, June 2015.

[10] M. H. Bollen, "Algorithms for characterizing measured three-phase unbalanced voltage dips," *IEEE Transactions on Power Delivery*, vol. 18, no. 3, pp. 937–944, July 2003.

[11] M. H. Bollen and E. Styvaktakis, "Characterization of three-phase unbalanced dips (as easy as one-two-three?)," *in Proceedings of the 2000 IEEE PES Summer meeting, Orlando (USA)*, vol. 1, pp. 81–86, October 2000.

[12] L. Zhan and M. H. Bollen, "Characteristic of voltage dips (sags) in power systems," *IEEE Transactions on Power Delivery*, vol. 15, no. 2, pp. 827–832, April 2000.

[13] M. Madrigal and B. Rocha, "A contribution for characterizing measured three-phase unbalanced voltage sags algorithm," *IEEE Transactions on Power Delivery*, vol. 22, no. 3, pp. 1885–1890, July 2007.

[14] Y. Amirat, M. E. H. Benbouzid, T. Wang, and S. Turri, "An ensemble empirical mode decomposition approach for voltage sag detection in a smart grid context," *International Review of Electrical Engineering*, vol. 8, no. 5, pp. 1503–1508, October 2013.

[15] M. H. Bollen, *Understanding Power Quality Problems*, vol. 3. IEEE Press New York, October 1999.

[16] V. Ignatova, P. Granjon, and S. Bacha, "Space vector method for voltage dips and swells analysis," *IEEE Transactions on Power Delivery*, vol. 24, no. 4, pp. 2054–2061, October 2009.

[17] B. Bizjak and P. Planinšič, "Classification of power disturbances using fuzzy logic," in *Proceedings of the 2006 IEEE IPEMC, Shanghai (China)*, pp. 1356–1360, September 2006.

[18] L. Saikia, S. Borah, and S. Pait, "Detection and classification of power quality disturbances using wavelet transform, fuzzy logic and neural network," in *Proceedings of the 2010 IEEE INDICON, Kolkata (India)*, pp. 1–5, December 2010.

[19] W. Kanitpanyacharoean and S. Premrudeepreechacharn, "Power quality problem classification using wavelet transformation and artificial neural networks," in *Proceedings of the 2004 IEEE PES PSCE, New York (USA)*, pp. 1496–1501, October 2004.

[20] H. He and J. A. Starzyk, "A self-organizing learning array system for power quality classification based on wavelet transform," *IEEE Transactions on Power Delivery*, vol. 21, no. 1, pp. 286–295, January 2006.

[21] P. G. Axelberg, I. Y.-H. Gu, and M. H. Bollen, "Support vector machine for classification of voltage disturbances," *IEEE Transactions on Power Delivery*, vol. 22, no. 3, pp. 1297–1303, July 2007.

[22] J. Huang, M. Negnevitsky, and T. D. Nguyen, "A neural-fuzzy classifier for recognition of power quality disturbances," *IEEE Transactions on Power Delivery*, vol. 17, no. 2, pp. 609–616, April 2002.

[23] M. Negnevitsky, V. Faybisovich, S. Santoso, E. Powers, W. Grady, and A. Parsons, "Discussion of "power quality disturbance waveform recognition using wavelet-based neural classifier-part 1: theoretical foundation"," *IEEE Transactions on Power Delivery*, vol. 15, no. 4, pp. 1347–1348, October 2000.

[24] P. Stoica, H. Li, and J. Li, "Amplitude estimation of sinusoidal signals: Survey, new results, and an application," *IEEE Transactions on Signal Processing*, vol. 48, pp. 338–352, February 2000.

[25] IEEE, *IEEE Standard Definitions for the Measurement of Electric Power Quantities Under Sinusoidal, Nonsinusoidal, Balanced, or Unbalanced Conditions*. IEEE Press, March 2010.

[26] P. Stoica and R. L. Moses, *Introduction to Spectral Analysis*, vol. 1. Prentice hall Upper Saddle River, February 1997.